Highly Efficient Light Harvesting of Eu(III) Complex in a Host-Guest Film by Triplet Sensitization

Shiori Miyazaki, [1] Kenichi Goushi,[2,3] Yuichi Kitagawa,[4,5] Yasuchika Hasegawa,[4,5] Chihaya Adachi,[2,3] Kiyoshi Miyata,[1]* and Ken Onda[1]*

[1] Department of Chemistry, Kyushu University, 744 Motooka, Nishi, Fukuoka 819-0395, Japan.

[2] Center for Organic Photonics and Electronics Research (OPERA), Kyushu University, 744 Motooka, Nishi, Fukuoka 819-0395, Japan.

[3] International Institute for Carbon Neutral Energy Research (I2CNER), Kyushu University, 744 Motooka, Nishi, Fukuoka 819-0395, Japan.

[4] Faculty of Engineering, Hokkaido University, N13W8, Kita-ku, Sapporo, Hokkaido 060-8628, Japan.

[5] Institute for Chemical Reaction Design and Discovery (WPI-ICReDD), Hokkaido University, N21 W10, Kita-ku, Sapporo, Hokkaido 001-0021, Japan.

*Corresponding author. E-mail: kmiyata@chem.kyushu-univ.jp (K.M.); konda@chem.kyushu-univ.jp (K.O.)

Abstract:

Lanthanide complexes are attractive light emitters owing to their ideal high color purity. Sensitization using ligands with high absorption efficiency is a powerful approach to enhancing photoluminescence intensity. However, the development of antenna ligands that can be used for sensitization is limited due to difficulties in controlling the coordination structures of lanthanides. Here, we demonstrate a system comprising triazine-based host molecules and $Eu(hfa)_3(TPPO)_2$ (hfa: hexafluoroacetylacetonato, TPPO: triphenylphosphine oxide), which shows drastically improved total photoluminescence intensity compared to conventional luminescent Eu(III) complexes. Time-resolved spectroscopic studies revealed that the energy transfer from the host molecules to Eu(III) occurs via the triplet states over several molecules with nearly unity efficiency. Our discovery paves the way for efficient light harvesting of Eu(III) complexes with simple fabrication using a solution process.

Main text:

Introduction

Molecule-based light-emission technologies have been intensively developed over the last few decades owing to their various applications, such as display panels, bioimaging sensors, optical telecommunications, and laser diodes[1-3]. Light-emitting materials must emit narrow-band light to achieve high color purity in their applications. However, general organic molecular emitters exhibit broadband emissions with a full width at a half-maximum (FWHM) of 70–100 nm. Trivalent lanthanide (Ln(III)) complexes exhibit narrow-band emissions with FWHMs of 10–20 nm caused by transitions between f-orbitals in Ln(III) that are shielded by electrons in the occupied 5s, 5p orbitals[4]; however, photoexciting the Laporte-forbidden f–f transition in Ln(III) directly with a small absorption coefficient (ε < 10 M^{-1} cm^{-1}) is difficult[5]. Many efforts have been made to overcome this difficulty by synthesizing organic ligands with large absorption coefficients and appropriate energy levels, which play an important role in efficient photosensitizers and intra-molecular ligand-to-Ln(III) energy transfer in complexes[6-8].

The overall photoluminescence (PL) intensity (I_{PL})[9,10] of an Ln(III) complex in a dilute solution or thin film is expressed as

$$I_{PL} = \varepsilon_{ligands} \times \phi_{tot} \quad (1)$$

where $\varepsilon_{ligands}$ and ϕ_{tot} represent the sum of all ligand absorption coefficients and the overall luminescence quantum yield of Ln(III) from ligand photoexcitation via intra-molecular energy transfer, respectively. This equation indicates that high PL intensity requires high light-absorption ability and luminescence quantum yield. $Eu(III)(hfa)_3(DPPTO)_2$ (hfa: hexafluoroacetylacetonato, DPPTO: 2-ddiphenyl phosphoryl triphenylene Fig. S1) is one of the Ln(III) complexes with the highest luminescence intensity in solution, I_{PL} = 90,000 $M^{-1}cm^{-1}$. The following three factors contribute to this high I_{PL}: (i) high $\varepsilon_{ligands}$ = 170,000 M^{-1} cm^{-1} of the two DPPTO ligands owing to their triphenylene chromophores[11], (ii) high ϕ_{tot} = 0.53 owing to suppression of nonradiative decay due to low vibrational frequencies of the phosphine-oxide linker in the DPPTO ligand and CF bonds in the hfa ligand[12-16], and (iii) enhancement of transition intensities in Eu(III) due to the asymmetric structure[17-21] formed by the hfa and DPPTO ligands. However, further improvement of luminescence intensity by designing new ligands is limited due to the difficulty in synthesizing ligands that simultaneously contain multiple

chromophores with a large absorption coefficient and stable coordination to Ln(III) compared to general transition metal ions.

Here, we propose that the host-guest system comprising π-conjugated molecules and Ln(III) complex emitters is an ideal system to dramatically improve the PL intensity of Ln(III) complexes with simple fabrication. In this system, multiple π-conjugated molecules with high absorption coefficients work as antennas for photosensitizing Ln(III) complexes; thus, a much higher absorption coefficient, denoted by $\varepsilon_{\mathrm{hosts}}$ in this case, is expected in Eq. (1) compared to the molecular Ln(III) complex. Moreover, it is not necessary to design linkers to coordinate with Ln(III). However, to achieve high ϕ_{tot}, such a host-guest system must overcome additional challenges; not only intra-molecular energy transfer but also inter-molecular energy transfer processes from host molecules to the Ln(III) complex are involved, and each process must be highly efficient. To achieve a very high I_{PL} for the host-gust system, it is essential to understand the mechanisms of the entire energy transfer process and design lossless energy transfer processes. Focusing on those issues, we chose a simple Eu(III) complex, Eu(III)(hfa)$_3$(TPPO)$_2$ (TPPO: triphenylphosphine oxide)[22,23], in which intra-molecular energy transfer occurs from the hfa ligands. We discovered that a host-guest system composed of a 2,4,6-tris(biphenyl-3-yl)-1,3,5-triazine (mT2T) host and the Eu(III) complex achieves an I_{PL} three orders of magnitude greater than the I_{PL} of the Eu(III) complex itself and that ~40 host molecules work for light harvesting of one Eu(III) complex via lossless triplet–triplet inter-molecular energy transfer.

In general, host-guest systems of Ln(III) complexes have been fabricated for an emitting layer in organic light-emitting diodes (OLEDs)[24-26]. Host molecules are known to affect the emission properties of Ln(III) complexes. Pietraszkiewicz *et al.* fabricated a 5 wt% Eu(nta)$_3$SFXPO-complex-doped host-guest film (nta:1-(2-naphthoyl)-3,3,3-trifluoroacetonate, SFXPO: spiro-fluorene-xanthene diphosphine oxide) with a higher PL quantum yield (PLQY) of 0.86 than 0.64 in a neat film[27]. This shows that host-guest systems may improve the efficiency of energy transfer processes compared to molecular Ln(III) complexes. Nonetheless, there are no design strategies apart from matching the energy of their lowest excited states[28-32], and there are few direct observations of inter- and intra-molecular energy transfer processes in host and guest systems[33-37].

We fabricated 10 wt% Eu(hfa)$_3$(TPPO)$_2$-doped films with the five host molecules demonstrated below, and a polymethyl methacrylate (PMMA) polymer with no photosensitization ability. We measured their I_{PL} and discovered that the mT2T host molecule exhibited the highest I_{PL} = 3,900,000 $\mathrm{M^{-1}\,cm^{-1}}$, which was approximately five hundred times larger than the PMMA host (Fig. 1). To explore the origin of the quite high I_{PL}, we investigated the emission mechanisms of the host-guest film using time-resolved photoluminescence spectroscopy (TR-PL) and femtosecond transient absorption spectroscopy (fs-TAS) in the multi-scale temporal range from sub-picoseconds to hundreds of microseconds. Beginning with the initial excitation of the host molecules and ending with the emission of the Eu(III) complex, we elucidated the mechanisms of all processes in the film: (1) the intersystem crossing (ISC) in the host molecule, (2) the inter-molecular energy transfer process from the host molecules to the ligands of the guest Eu(III) complex, (3) the intra-molecular energy transfer process from the ligands to

Eu(III), and (4) the emission processes of f–f transitions in Eu(III). Furthermore, we discovered that the yields of all energy transfer processes, (1)–(3), were nearly unity and that the yield of the Eu(III) emission process (4) determined the overall quantum yield of the film. This highly efficient PL is attributed to the ideal triplet sensitization processes: rapid and efficient ISC in mT2T leads to efficient triplet–triplet inter-molecular energy transfers without any losses.

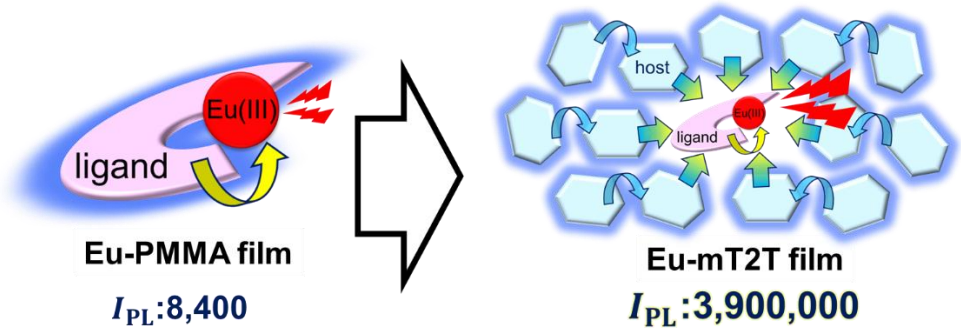

Fig. 1. Drastic improvement of the overall photoluminescence intensity (I_{PL}) by efficient photosensitization from many host molecules. Schematic view of photo-sensitization by intra-molecular energy transfer from the ligands to Eu(III) in the $Eu(hfa)_3(TPPO)_2$-doped PMMA film (Eu-PMMA film, left) and light harvesting by inter-molecular energy transfer from many hosts to Eu(III) in the $Eu(hfa)_3(TPPO)_2$-doped mT2T film (Eu-mT2T film, right).

Results and Discussion

Contribution of host molecules to I_{PL}

Five different host molecules were used to fabricate $Eu(hfa)_3(TPPO)_2$-doped films: mT2T, 2-(9,9'-spirobi[fluoren]-3-yl)-4,6-diphenyl-1,3,5-triazine (SF3TRZ), 3,3′-di(9*H*-carbazol-9-yl)biphenyl (mCBP), 4,4′-*N,N*′-dicarbazole-biphenyl (CBP), and 2,4,6-tris(1,1′-biphenyl-4-yl)-[1,3,5]triazine (T2T) (Fig. 2, S2). These host molecules have been used in conventional OLED applications. To evaluate the intrinsic optical properties of isolated $Eu(hfa)_3(TPPO)_2$, we also fabricated an $Eu(hfa)_3(TPPO)_2$-doped PMMA (Eu-PMMA) film. Because PMMA is transparent in the >250 nm range[38], the absorption spectrum of the Eu-PMMA film in the >250 nm range is identical to that of $Eu(hfa)_3(TPPO)_2$. The absorption range of 250–350 nm for isolated $Eu(hfa)_3(TPPO)_2$ is primarily assigned to the S_0–S_n transition of the hfa ligands[39], and the absorption of TPPO in this range is much weaker (Fig. S3A). The host-guest systems significantly enhanced their overall absorption coefficients because all of the host molecules have higher absorption coefficients in the range of 250–280 nm than the hfa ligands (Table 1, Fig. S3B).

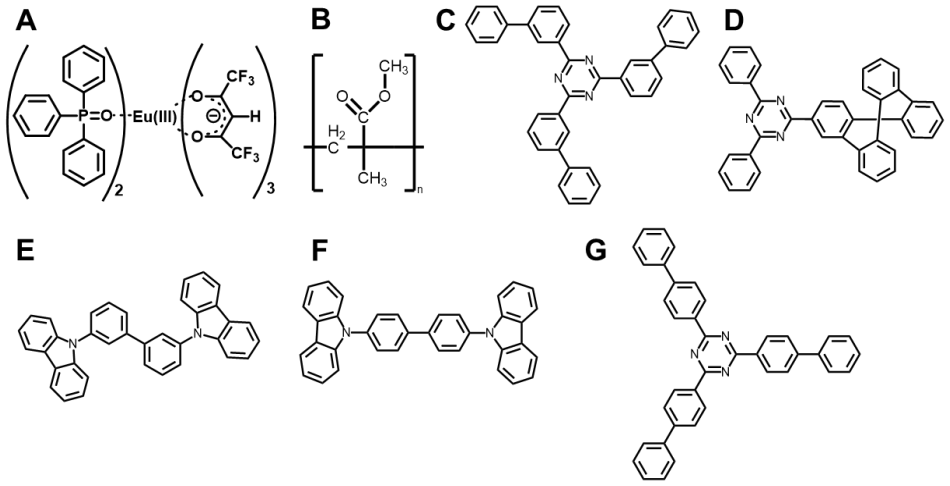

Fig. 2. Chemical structures. (A) $Eu(hfa)_3(TPPO)_2$, **(B)** PMMA, **(C)** mT2T, **(D)** SF3TRZ, **(E)** mCBP, **(F)** CBP, and **(G)** T2T.

To investigate the sensitization ability of the host molecules, we compared the PL properties of the host-guest films to those of the Eu-PMMA film (Fig. 3A). After photoexciting the Eu-PMMA film with 315 nm light, emission bands from Eu(III) were observed at 581, 594, 615, 654, and 701 nm (Fig. S4) and are assigned to the transitions $^5D_0 \rightarrow {}^7F_J$ and J = 0, 1, 2, 3, and 4, respectively[4]. Since the excitation at 315 nm selectively excites the hfa ligands (Fig. S3A), the Eu(III) sensitization by the hfa ligands in the Eu-PMMA film was confirmed. Also, after photoexcitation with 260–267 nm light, the same emission bands in Eu(III) were observed in all of the host-guest films (Fig. 3B, S5). Given that the absorption coefficients of the host molecules in this wavelength range are much larger than those of the guest complex (Fig. S3), this indicates that inter-molecular energy transfer from the host molecules to Eu(III) occurs in all host-guest films.

The sensitization efficiencies of the host-guest films are discussed qualitatively based on their emission spectra. A broad emission band located at around 400 nm was observed for $Eu(hfa)_3(TPPO)_2$-doped SF3TRZ (Eu-SF3TRZ), mCBP (Eu-mCBP), CBP (Eu-CBP), and T2T (Eu-T2T) films, in addition to the emission from Eu(III) (Fig. S5). These bands were assigned to the fluorescence from the lowest singlet excited state (S_1) of each host molecule (Fig. S6), indicating imperfect energy transfer to the Eu(III) complex. In contrast, no host molecule emission band was observed in the $Eu(hfa)_3(TPPO)_2$-doped mT2T (Eu-mT2T) film (Fig. 3B). This result suggests that inter-molecular energy transfer from the host mT2T molecules to the Eu(III) complex occurs extremely efficiently in the film. In fact, ϕ_{tot} of Eu-mT2T (ϕ_{tot} = 0.84) was significantly higher than Eu-PMMA (ϕ_{tot} = 0.60) (Table 1). The efficient sensitization is further supported by the excitation spectra probed at the Eu(III) emission coincided with the absorption spectra of these films (Fig. 3B, 3C).

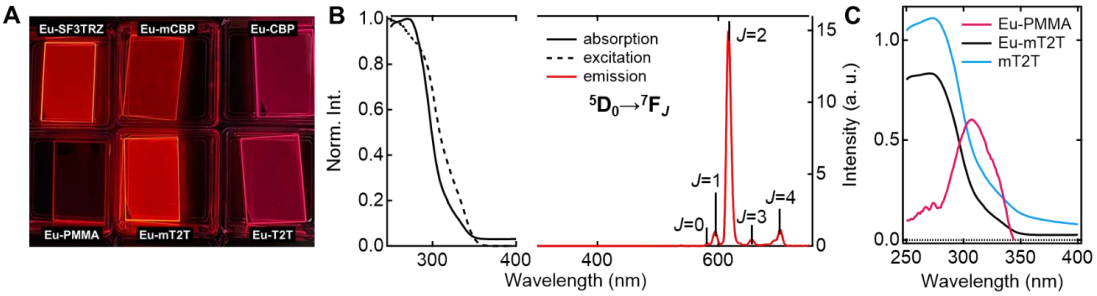

Fig. 3. Optical properties of Eu(hfa)$_3$(TPPO)$_2$-doped films. (A) Photos of emission from the fabricated films upon photoexcitation with 254 nm. **(B)** Absorption (solid line), excitation probed at 615 nm (broken line), and emission (red line) spectra of the Eu-mT2T film. **(C)** Absorption spectra of the Eu-PMMA film (pink line), Eu-mT2T film (black line), and mT2T neat film (sky blue line).

To estimate the number of host molecules that contributed to one Eu(III) emission, we measured the photophysical properties of the Eu-mT2T films with different doping ratios of Eu(III) complex to mT2T (Table 1). As a results, ϕ_{tot} was independent of the mixing ratio in the 10–50% range, implying that approximately ten host molecules contributed to the emission of one Eu(III) complex via energy transfer between the host and guest molecules. Considering this result, I_{PL} of host-guest films can be expressed as

$$I_{\mathrm{PL}} = \varepsilon_{\mathrm{hosts}} \times \phi_{\mathrm{tot}} = \varepsilon_{\mathrm{host}}^{\mathrm{mol}} \times n_{\mathrm{host}} \times \phi_{\mathrm{tot}} \qquad (2)$$

where $\varepsilon_{\mathrm{host}}^{\mathrm{mol}}$ and n_{host} represent the molar absorption coefficient of the host molecule and the number of host molecules that contributed to one Eu(III) emission, respectively. The I_{PL} is plotted as a function of n_{host} in Fig. 4. The I_{PL} for the Eu(hfa)$_3$(TPPO)$_2$-doped films increases monotonically even when n_{host} = 40, indicating that more than 40 host molecules work as photosensitizers for one Eu(III) complex. Note that the maximum I_{PL} is more than one order of magnitude higher than that of the conventional highly luminescent complex Eu(hfa)$_3$(DPPTO)$_2$[11].

Table 1. Absorption and emission properties of the Eu(hfa)$_3$(DPPTO)$_2$ and Eu(hfa)$_3$(TPPO)$_2$-doped films. The values of $\varepsilon_{\mathrm{host}}^{\mathrm{mol}}$ and $\varepsilon_{\mathrm{ligands}}$ of Eu(hfa)$_3$(DPPTO)$_2$-PMMA film were evaluated at 267 nm. The values of $\varepsilon_{\mathrm{ligands}}$ of Eu(hfa)$_3$(TPPO)$_2$-PMMA film was evaluated at 315 nm. I_{PL} was calculated using eq. (1) and eq. (2). The PLQYs (ϕ_{tot}) were measured each photoexcitation wavelength (λ_{ex}) ($\varepsilon_{\mathrm{ligands}}$, $\varepsilon_{\mathrm{host}}^{\mathrm{mol}}$, n_{host}, I_{PL}; see text for details).

guest	host	Eu conc. /wt%	$\boldsymbol{\varepsilon_{\mathrm{ligands}}}$ /M^{-1}cm^{-1}	$\boldsymbol{\varepsilon_{\mathrm{host}}^{\mathrm{mol}}}$ /M^{-1}cm^{-1}	$\boldsymbol{n_{\mathrm{host}}}$	$\boldsymbol{\phi_{\mathrm{tot}}}$	$\boldsymbol{\lambda_{\mathrm{ex}}}$ /nm	$\boldsymbol{I_{\mathrm{PL}}}$ /M^{-1}cm^{-1}
Eu(hfa)$_3$(DPPTO)$_2$	PMMA	10	1.7×10^5	-	-	0.55	267	9.4×10^4
Eu(hfa)$_3$(TPPO)$_2$	PMMA	10	1.4×10^4	-	-	0.60	315	8.4×10^3
	mT2T	5 10 30 50	-	1.0×10^5	47 22 5.8 2.5	0.76 0.84 0.83 0.78	267	3.9×10^6 1.9×10^6 4.8×10^5 2.1×10^5
	SF3TRZ	10	-	1.1×10^5	22	0.76	267	1.9×10^6
	mCBP	10	-	4.6×10^4	25	0.33	267	3.8×10^5
	CBP	10	-	4.0×10^4	25	0.29	267	2.6×10^5
	T2T	10	-	1.2×10^4	22	0.16	267	4.4×10^4

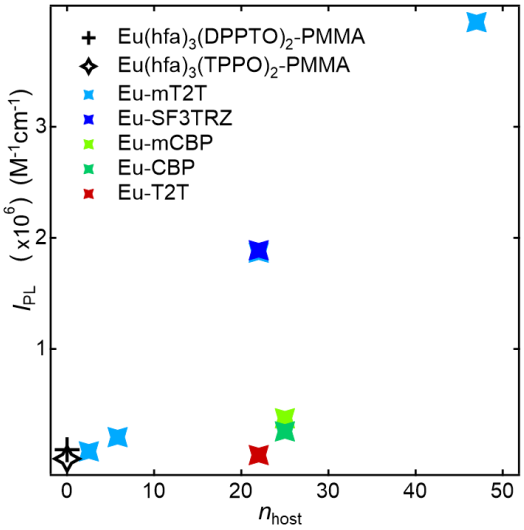

Fig. 4. Host and its ratio dependence of overall luminescence intensities (I_{PL}). I_{PL} of $Eu(hfa)_3(DPPTO)_2$-doped PMMA film (black plus marker), $Eu(hfa)_3(TPPO)_2$-doped PMMA film (black cross marker), Eu-mT2T film (sky blue star markers), Eu-SF3TRZ film (blue star marker), Eu-mCBP film (yellow green star marker), and Eu-T2T film (red star marker), calculated using Eq. (1) and Eq. (2). n_{host} is the number of host molecules contributed to one Eu(III) emission.

Initial process after photoexcitation: rapid and efficient ISC in mT2T

Understanding the mechanisms of intra- and inter-molecular energy transfer processes requires understanding the photophysical processes occurring within host molecules. To investigate the processes in the time domain, we measured and compared the fs-TAS spectra of the Eu-mT2T film (Fig. 5A) and the mT2T neat film (Fig. S7A). The absorbance change (ΔAbs.) of the Eu-mT2T film increased in the <600 nm range, whereas it decreased in the >600 nm range, with an isosbestic point at 600 nm. We performed a global analysis of the fs-TAS spectra, assuming a sequential model with two components because the isosbestic point indicates an exclusive transition between two states[40]. With a time constant of 71.2 ± 0.6 ps, the first component was converted to the second component (Fig. 5B). The evolution associated spectra (EAS) and concentration kinetics of the two components are shown in Fig. 5C and 5D, respectively. We analyzed the fs-TAS of the mT2T neat film in the same way to assign the observed species. The global analysis also resulted in similar EASs (Fig. S7C), with a time constant of 44.9 ± 0.4 ps (Fig. S7D). The two EAS components were reasonably assigned to S_1 and the lowest triplet excited state (T_1) in the case of the neat film, and the time constant represented the ISC rate. Therefore, the two components observed in the Eu-mT2T film were assigned to S_1 and T_1 of the host mT2T molecule. These time constants are much faster than those of the ISC process for aromatic organic molecules in general, which can be explained by the presence of lone pairs in the triazine moieties in mT2T accelerating the ISC rate[41,42]. We conclude that mT2T undergoes a rapid and nearly unity ISC before exciton diffusion and energy transfer in the host-guest film.

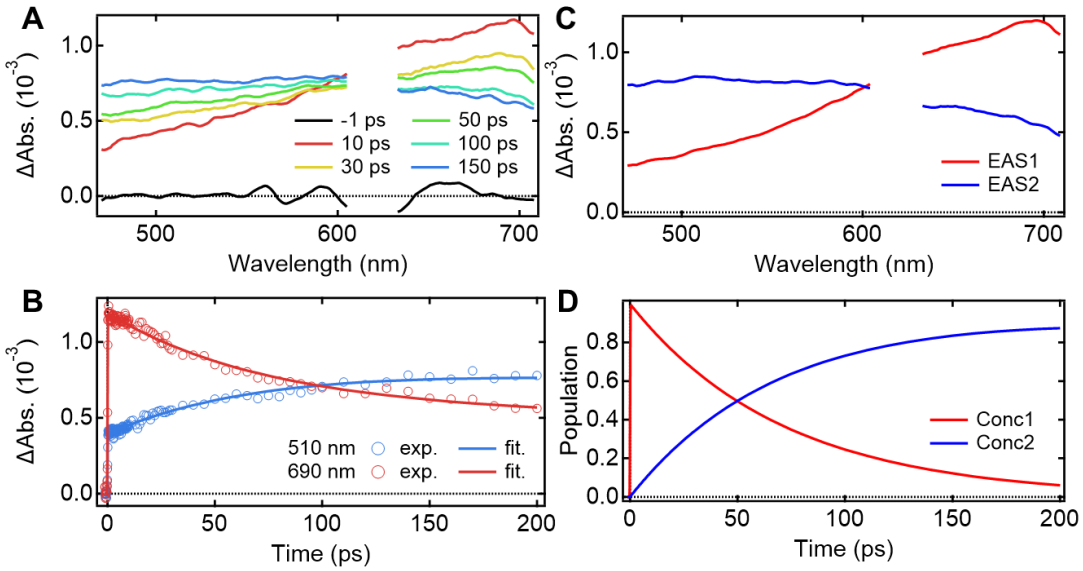

Fig. 5. fs-TAS spectra and the results of their global analysis for the Eu-mT2T film. **(A)** Temporal evolutions of the fs-TAS spectra after photoexcitation at 267 nm. **(B)** Temporal profiles of the fs-TAS spectra at 510 nm (blue circles) and 690 nm (red circles) and corresponding fitting curves resulted from the global analysis. **(C)** EAS. **(D)** Corresponding concentration kinetics were obtained from the global analysis.

Quantum yields of each energy transfer process

Given that rapid ISC occurs first in the host film, Fig. 6 shows the predicted energy transfer processes in the Eu-mT2T film after photoexcitation. We first estimated the luminescence quantum yield of Eu(III) (ϕ_{Eu}) in the host-guest films to estimate the quantum yield of each process. The natural radiative rate constant of Eu(III) ($k_{\mathrm{r}}^{\mathrm{Eu}}$) can be calculated from the ratio of the electric dipole transition ($^5D_0 \rightarrow {}^7F_{0,\,2,\,3,\,4}$) to the magnetic dipole transition ($^5D_0 \rightarrow {}^7F_1$) in the observed emission spectrum of Eu(III) (Fig. 3B, Eq. (S1); see the supplemental text for details)[43]. ϕ_{Eu} is also determined by the ratio of $k_{\mathrm{r}}^{\mathrm{Eu}}$ to the observed rate constant of the $^5D_0 \rightarrow {}^7F_2$ transition ($k_{\mathrm{obs}}^{\mathrm{Eu}}$) (Eq. (S2) and (S3)). The estimated ϕ_{Eu}, rate constants, and parameters are summarized in Table S1. We calculated η_{sens} because ϕ_{tot} represents the product of ϕ_{Eu} and overall photosensitization efficiency (η_{sens}; Eq. (S4); Table S1). Note that η_{sens} in the 10 wt% Eu-mT2T film is nearly unity, with $\eta_{\mathrm{sens}}^{\mathrm{Eu-mT2T}}$ = 0.97. This indicates almost perfect sensitization of photoexcited mT2T to Eu(III) in the Eu-mT2T film, which is more efficient than sensitization of hfa ligands in the Eu-PMMA film, $\eta_{\mathrm{sens}}^{\mathrm{Eu-PMMA}}$ = 0.71.

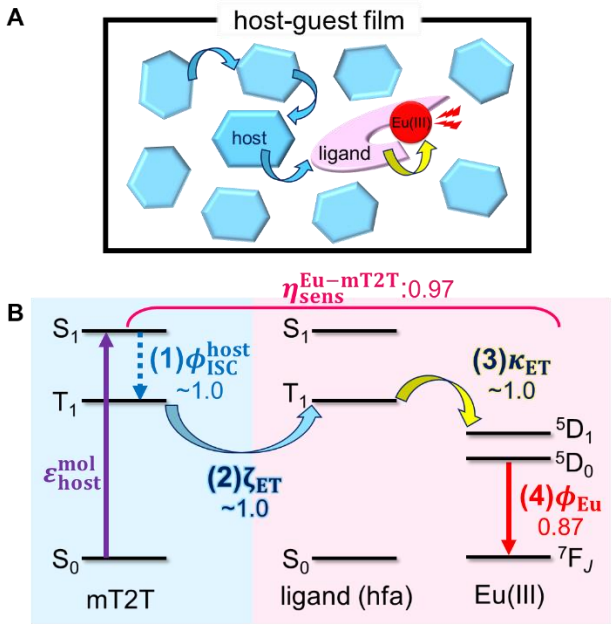

Fig. 6. Overview of inter- and intra-molecular energy transfer processes in the Eu-mT2T film. (A) Schematic in real space. **(B)** Schematic in energy levels. ϕ_{ISC}^{host}, ζ_{ET}, κ_{ET}, ϕ_{Eu} represent the quantum yields of (1) ISC in mT2T, (2) inter-molecular energy transfer from mT2T to the hfa ligands, (3) intra-molecular energy transfer from the hfa ligands to Eu(III), and (4) the emission in Eu(III), respectively. $\eta_{sens}^{Eu-mT2T}$ is the overall photosensitization efficiency in the Eu-mT2T film (Eq. (4)).

To identify the factor that improves energy transfer efficiency in the Eu-mT2T film, we compared the sensitization efficiencies of intra-molecular energy transfer in the Eu-PMMA film ($\eta_{sens}^{Eu-PMMA}$) and the inter- and intra-molecular energy transfer in the Eu-mT2T film ($\eta_{sens}^{Eu-mT2T}$). $\eta_{sens}^{Eu-PMMA}$ is expressed as follows:

$$\eta_{sens}^{Eu-PMMA} = \phi_{ISC}^{ligand} \times \kappa_{ET} \quad (3)$$

where ϕ_{ISC}^{ligand} and κ_{ET} represent the ISC yield of the ligand and the efficiency of intra-molecular energy transfer, respectively. In contrast, $\eta_{sens}^{Eu-mT2T}$is expressed as

$$\eta_{sens}^{Eu-mT2T} = \phi_{ISC}^{host} \times \zeta_{ET} \times \kappa_{ET} \quad (4)$$

where ϕ_{ISC}^{host} and ζ_{ET} represent the yield of ISC of the host and the efficiency of inter-molecular energy transfer, respectively. Fig. 6B shows the symbols for the Eu-mT2T film. We conducted time-resolved measurements in $Eu(hfa)_3(TPPO)_2$-doped neat (Eu-neat) and $Gd(hfa)_3(TPPO)_2$-doped neat (Gd-neat) films to estimate the κ_{ET} of the Eu(III) complex (Fig. S8, S9). We can observe intrinsic emission from the hfa ligands in the Gd-neat film because there is no intra-molecular energy transfer to Gd(III) due to the energy level mismatch (Fig. S9A, B, C). We compared the time constants of the fs-TAS and TR-PL measurements to analyze each time constant in the energy transfer process (Fig. S10).

The κ_{ET} of the Eu(III) complex was >0.99 when the lifetimes of the T_1 ligands between in the Eu-neat film and the Gd-neat film were compared (Table S2, Eq. (S5)). We conclude that the quantum yield of the ISC at the ligands, ϕ_{ISC}^{ligand}, in the Eu-PMMA film is the dominant factor in the relatively low $\eta_{sens}^{Eu-PMMA}$. Sensitization processes in the case of the Eu-mT2T film, in contrast, occur via inter-molecular energy transfer via T_1 states between the mT2T and hfa ligands. Because the quantum yield of ISC in mT2T is nearly unity, the Eu-T2T film achieves more efficient sensitization.

Time-domain view of the whole sensitization processes

Multiscale TR-PL measurements were performed to quantify energy transfer processes in the time domain. The pseudo-2D color plot of the TR-PL of the Eu-mT2T film after photoexcitation at 267 nm is shown in Fig. 7A–C. Following photoexcitation, a broad emission band in the 350–500 nm range was observed (Fig. 7A, 7D). This band shape is approximately identical to the fluorescence observed in the mT2T neat film (Fig. S11); this emission is attributed to the S_1 emission in the mT2T. Note that no emission from mT2T was observed in the steady-state emission spectrum (Fig. 3B) because its time-integrated intensity was much smaller than that of Eu(III). The decay time constant of mT2T emission was estimated to be <100 ps (Fig. 7G), which agrees with the time constant of ISC in mT2T (~70 ps) estimated from fs-TAS spectra.

Following the rapid decay of the fluorescence from mT2T, narrow-band emissions in the nanosecond to microsecond time range were observed (Fig. 7B, 7C, 7E, 7F). According to Dicke's diagram, all of these emission bands were assigned to the f–f transitions in Eu(III)[44]. The 535, 555, and 585 nm bands in the nanosecond region (Fig. 7A, 7E) were assigned to the transitions $^5D_1 \rightarrow {}^7F_1$, $^5D_1 \rightarrow {}^7F_2$, and $^5D_1 \rightarrow {}^7F_3$, respectively. The bands at 590 and 615 nm in the microsecond region (Fig. 7B, 7F) were assigned to $^5D_0 \rightarrow {}^7F_1$ and $^5D_0 \rightarrow {}^7F_2$, respectively. The rise time constant of the $^5D_1 \rightarrow {}^7F_3$ transition was estimated to be 41.0 ± 0.8 ns (Fig. 7H), which is much longer than the time constant of the ISC in mT2T (<100 ps). This result indicates that the energy transfer to Eu(III) is ~40 ns and is mediated via the T_1 states.

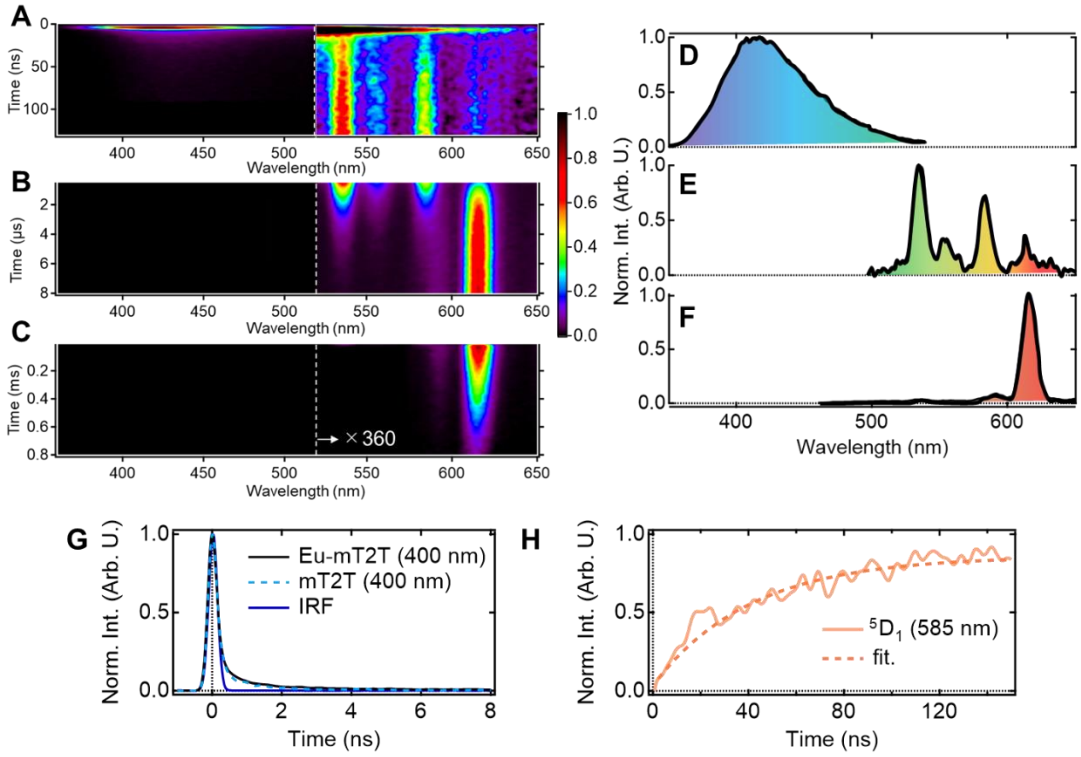

Fig. 7. TR-PL spectra and their temporal profiles. (A–C) Pseudo-2D plot of the emission from the Eu-mT2T film after photoexcitation at 267 nm in the time range of **(A)** 0–130 ns, **(B)** 0.5–8 μs, and **(C)** 0.01–0.8 ms. For clarity, the intensities above 520 nm are magnified by a factor of 360. **(D–F)** Normalized emission intensity spectra were obtained from the streak images by the time integration of **(D)** 0.05–0.15 ns, **(E)** 145–155 ns, and **(F)** 6.5–7.5 μs. **(G)** Temporal profiles of the emission at 400 nm after photoexcitation of the Eu-mT2T film (solid black line) and the mT2T neat film (broken sky blue line) together with the instrumental response function (IRF, solid blue line). **(H)** Temporal profiles of the emission at 585 nm subtracted the overlapped fluorescence of the host molecules after photoexcitation of the Eu-mT2T film (orange line) and fitting curve (broken orange line).

Mechanisms of efficient triplet-state mediated energy transfer and sensitization

Here, we discuss the origins of efficient inter-molecular energy transfer in the Eu-mT2T film in terms of T_1 energy matching. We compared the T_1 energies of the mT2T molecule to those of the hfa ligands of the Eu(III) complex. The T_1 energies for mT2T and hfa were estimated from the phosphorescence spectra (Fig. S12) to be 2.66 and 2.70 eV, respectively. Due to the close proximity of the energies, an efficient energy transfer from mT2T to the Eu(III) complex is anticipated. We also compared the T_1 energies of the other host molecules to those of hfa, confirming that energetically resonant conditions in the T_1 energies of the host and hfa are important for the higher PLQYs in the host-guest films (Fig. S12G). This indicates that inter-molecular energy transfer from host molecules to Eu(III) occurs via the T_1 of hfa. Furthermore, the phosphorescence of hfa ligands was observed following energy transfer from T_1 in mT2T (Fig. S12A, S13) in the $Gd(hfa)_3(TPPO)_2$-doped mT2T (Gd-mT2T) film, confirming efficient host-to-hfa energy

transfer. We concluded that the energy resonance in T_1 between mT2T and hfa causes highly efficient inter-molecular energy transfer sensitization (ζ_{ET} ~1.0).

Finally, we discuss triplet exciton diffusion in the host matrix by comparing energy transfer to Eu(III) and PLQYs in Eu-mT2T films with different mT2T and Eu(III) complex ratios (Fig. S14, Table S3). As the concentration of the Eu(III) complex increased, so did the rise time constant of $^5D_1$ (Fig. S14). The rise time constant of the low ratio of the mT2T (Eu(III) concentration of 50 wt%) film exhibits the fastest rise time constant (~29 ns). Because the lifetime of T_1 in mT2T is likely to be much longer than the diffusion time scale, sensitization processes mediated by triplet–triplet energy transfer are effective in realizing ideal sensitization for Eu(III) emission.

Summary

We demonstrated highly efficient light harvesting of Eu(III) in complex-doped host-guest films with $Eu(hfa)_3(TPPO)_2$. We achieved an extremely large improvement in the luminescence intensity of Eu(III) when we used mT2T, which is a one of the triazine derivatives that works as a good energy harvesting antenna. After photoexcitation to Eu(III) emission, we estimated the quantum yields of all energy transfer processes and discovered that all energy transfer processes occur with almost unity quantum yield. We conclude from the TR-PL and fs-TAS measurements that efficient energy transfer occurs via resonant energy transfer from T_1 of mT2T to T_1 of hfa following rapid and highly efficient ISC in mT2T. This mechanism can avoid energy loss in the ISC process in the hfa ligands of an Eu(III) complex and overcome the intrinsic limitations of conventional direct sensitization by the ligands. Based on this result, we propose a novel light harvesting method for Ln(III) with simple fabrication: a host-guest film composed of host molecules with efficient ISC, which works as an efficient photosensitizer, and a guest Ln(III) complex with ligands having a T_1 state whose energy matches that of T_1 in the host, which works as an efficient energy accepter and emitter.

Materials and Methods

Materials

A previously reported procedure was used to synthesize $Eu(hfa)_3(TPPO)_2$ (*22*). mT2T, SF3TRZ, and mCBP were purchased from the NARD Institute Ltd. (Hyogo, Japan). CBP was purchased from Angene International Ltd. (Nanjing, China). T2T was purchased from Tokyo Chemical Industry Co., Ltd. (Tokyo, Japan). mT2T, SF3TRZ, mCBP, and CBP were purified via sublimation. Chloroform, dichloromethane, and methanol were purchased from Kanto Kagaku Co., Ltd. (Tokyo, Japan). Without further purification, all solvents were used as received.

Fabrication of thin films

Thin films for optical measurements were fabricated by spin-coating on quartz substrates. The quartz substrates were washed by ultrasonic cleaning with acetone and isopropanol. For the preparation of neat films, the emitter compounds were dissolved in chloroform (10 wt%). To prepare the host-guest films, a weight ratio of 1:9 of the guest molecule and the host molecule was dissolved in chloroform to obtain an overall concentration of 10 wt%. Before use, the solution was filtered through a 0.2 μm filter, and the quartz

substrates were heated to 80 °C. The solution was spin-coated onto quartz substrates for 60 s at 1000 rpm and then annealed at 70 °C for 10 min. Table S4 shows the thicknesses of the films.

Thin films for refractive index measurements were fabricated on silicon substrates using vacuum vapor deposition at a pressure of less than 10^{-3} Pa. We used a fixed deposition rate of 0.5 nm/s and a thickness of 100 nm.

General methods

UV-vis absorption spectra were measured using a PerkinElmer LAMDA950 spectrophotometer. Excitation and PL spectra of the $Eu(hfa)_3(TPPO)_2$-doped PMMA film (excitation wavelength for PL spectra: λ_{ex} = 315 nm and probe wavelength for excitation spectra: λ_{em} = 615 nm), $Eu(hfa)_3(TPPO)_2$-doped mT2T film (λ_{ex} = 267 nm, λ_{em} = 615 nm), $Eu(hfa)_3(TPPO)_2$-doped T2T film (λ_{ex} = 260 nm, λ_{em} = 615 nm), $Eu(hfa)_3(TPPO)_2$-doped SF3TRZ film (λ_{ex} = 267 nm, λ_{em} = 615 nm), $Eu(hfa)_3(TPPO)_2$-doped mCBP film (λ_{ex} = 267 nm, λ_{em} = 615 nm), and $Eu(hfa)_3(TPPO)_2$-doped CBP film (λ_{ex} = 260 nm, λ_{em} = 615 nm) were measured using spectrofluorometers (FP-8600, JASCO; PMA-12, Hamamatsu Photonics). The phosphorescence spectra of the neat films of $Gd(hfa)_3(TPPO)_2$, TPPO (λ_{ex} = 335 nm), $Gd(hfa)_3(TPPO)_2$-doped mT2T (λ_{ex} = 267 nm), mT2T (λ_{ex} = 267 nm), T2T (λ_{ex} = 315 nm), SF3TRZ (λ_{ex} = 267 nm), mCBP (λ_{ex} = 267 nm), and T2T (λ_{ex} = 267 nm) at 77 K were measured using a spectrofluorometer (FP-8600, JASCO; PMA-12, Hamamatsu Photonics).

The photoluminescence quantum yields were measured using a Hamamatsu Photonics Quantaurus-QY instrument equipped with an integrating sphere. A time-correlated single-photon counting lifetime spectroscopy system (HAMAMATSU Quantaurus-Tau C11367-21, C11567-02, and M12977-01) was used to PL measure lifetimes.

The refractive indexes and thicknesses of the films were measured using variable-angle spectroscopic ellipsometry (M-2000U, J. A. Woollam Co., Inc., United States).

Time-resolved photoluminescence (TR-PL)

TR-PL measurements were performed using a streak camera system (Hamamatsu C4780, time resolution <30 ps) synchronized with a Ti:sapphire regenerative amplifier (Spectra-Physics, Spitfire Ace, pulse duration = 120 fs, repetition rate = 1 kHz, pulse energy = 4 mJ/pulse, central wavelength = 800 nm)[34]. The samples were excited by the third harmonic of the fundamental pulse from an amplifier (267 nm). The polarization angle of the light for excitation and detection was set to the magic angle (54.7°)[45]. Before measuring, all films were encapsulated. The excitation energy was kept to less than 0.8 mJ/cm^2.

Femtosecond transient absorption spectroscopy (fs-TAS)

Transient absorption (TA) measurements were conducted using the pump-probe method[46]. The light source was a Ti:sapphire regenerative amplifier system (Spectra-Physics, Spitfire Ace, pulse duration = 120 fs, repetition rate = 1 kHz, pulse energy = 4 mJ/pulse, central wavelength = 800 nm) seeded by a Ti:sapphire femtosecond mode-locked laser (Spectra-Physics, Tsunami). The output of the amplifier was divided into two pulses for

the pump and probe. The samples were pumped by the third harmonic of the fundamental pulse from an amplifier (267 nm). The broadband probe pulse (450–750 nm) was generated using a sapphire crystal of 1 mm thickness. The angle between the pump and probe polarizations was set to the magic angle (~54.7 deg.). The pump and probe pulse beam sizes at the sample position were <0.7 mmϕ and <0.5 mmϕ, respectively. A PC-controlled mechanical delay state was used to adjust the delay time between the pump and probe pulses. The probe pulse that passed through the sample films was dispersed by a polychromator (JASCO, CT-10, 300 grooves/500 nm), and the spectra were captured using a multichannel detection system with a CMOS sensor (UNISOKU, USP-PSMM-NP). To avoid damage, all the films were encapsulated before being measured and were mechanically moved continuously. The excitation energy was kept to less than 0.4 mJ/cm^2. The recorded data was analyzed using a Python-based homemade program.

References

1. M. A. Baldo, O. F. O'Brien, Y. You, A. Shoustikov, S. Sibley, M. E. Thompson, S. R. Forrest, Highly efficient phosphorescent emission from organic electroluminescent devices. *Nature* **395**, 151-154 (1998).
2. H. Uoyama, K. Goushi, K. Shizu, H. Nomura, C. Adachi, Highly efficient organic light-emitting diodes from delayed fluorescence. *Nature* **492**, 234-238 (2012).
3. A. S. D. Sandanayaka, T. Matsushima, F. Bencheikh, S. Terakawa, W. J. Potscavage Jr., C. Qin, T. Fujihara, K. Goushi, J.-C. Ribierre, C. Adachi, Indication of current-injection lasing from an organic semiconductor. *Appl. Phys. Express* **12**, 061010 (2019).
4. K. Binnemans, Interpretation of europium(III) spectra. *Cood. Chem. Rev.* **295**, 1-45 (2015).
5. B. R. Judd, Optical absorption intensities of rare-earth ions. *Phys. Rev.* **127**, 750 (1962).
6. L. R. Melby, N. J. Rose, E. Abramson, J. C. Caris, Synthesis and fluorescence of some trivalent lanthanide complexes. *J. Am. Chem. Soc.* **86** (23), 5117-5125 (1964).
7. Y. Hasegawa, Y. Wada, S. Yanagida, Strategies for the design of luminescent lanthanide(III) complexes and their photonic applications. *J. Photochem. Photobiol. C Rev.* **5**, 183-202 (2004).
8. J. -C. G. Bünzli, On the design of highly luminescent lanthanide complexes. *Cood. Chem. Rev.* **293-294**, 19-47 (2015).
9. J. Yuan, K. Matsumoto, Fluorescence enhancement by electron-withdrawing groups on -diketones in Eu(III)-diketonato-topo ternary complexes. *Analytical Sciences* **12**, 31-36 (1996).
10. K.-L. Wong, J.-C. G. Bünzli, P. A. Tanner, Quantum yield, and brightness. J. Lumin. **224**, 117256 (2020).
11. Y. Kitagawa, F. Suzue, T. Nakanishi, K. Fushimi, Y. Hasegawa, A highly luminescent Eu(III) complex based on an electronically isolated aromatic ring system with ultralong lifetime. *Dalton Trans.* **47**, 7327-7332 (2018).
12. N. Filipescu, W. F. Sager, and F. A. Serafin, Substituent effects on intramolecular energy transfer. II. Fluorescence spectra of europium and terbium β-diketone chelates. *J. Phys. Chem.* **68**, 3324-3346 (1964).
13. S. Sato, M. Wada, Relations between intramolecular energy transfer efficiencies and triplet state energies in rare earth β-diketone chelates. *Bull. Chem. Soc. Jpn.* **43**, 1955-1962 (1970).

14. D. B. A. Raj, B. Francis, M. L. P. Reddy, R. R. Butorac, V. M. Lynch, A. H. Cowley, Highly luminescent poly(methyl methacrylate)-incorporated europium complex supported by a carbazole-based fluorinated β-diketonate ligand and a 4,5-bis(diphenylphosphino)-9,9-dimethylxanthene oxide co-ligand. *Inorg. Chem.* **49**, *19*, 9055-9063 (2010).
15. N. B. D. Lima, S. M. C. Gonçalves, S. A. Júnior, A. M. A. Simas, A comprehensive strategy to boost the quantum yield of luminescence of europium complexes. *Sci. Rep.* **3**, 1-8 (2013).
16. Y. Hasegawa, K. Murakoshi, Y. Wada, S. Yanagida, J. Kim, N. Nakashima, T. Yamanaka, Enhancement of luminescence of Nd^{3+} complexes with deuterated hexafluoroacetylacetonato ligands in organic solvent. *Chem. Phys. Lett.*, **248**, 8-12 (1996).
17. K. Miyata, T. Nakagawa, R. Kawakami, Y. Kita, K. Sugimoto, T. Nakashima, T. Harada, T. Kawai, Y. Hasegawa, Remarkable luminescence properties of lanthanide complexes with asymmetric dodecahedron structures. *Chem. Eur. J.* **17**, 521-528 (2011).
18. K. Nakamura, Y. Hasegawa, H. Kawai, N. Yasuda, N. Kanehisa, Y. Kai, T. Nagamura, S. Yanagida, Y. Wada, Enhanced lasing properties of dissymmetric Eu(III) complex with bidentate phosphine ligands. *J. Phys. Chem. A* **111**, 3029-3037 (2007).
19. P. A. Tanner, Some misconceptions concerning the electronic spectra of tri-positive europium and cerium. *Chem. Soc. Rev.* **42**, 5090-5101 (2013).
20. B. G. Vats, S. Kannan, M. Kumar, M. G. B. Drew, Ligand- field asymmetry-controlled luminescent europium (III) and samarium(III) tris(β-diketonate) complexes of diphenyl-(2-pyridyl-N-oxide)-phosphine oxide. *Chemistry Select* **2,** *13*, 3683-3689 (2017).
21. A. F. Kirby, D. Foster, F. S.Richardson, Comparison of $^7F_J \leftarrow ^5D_0$ emission spectra for Eu(III) in crystalline environments of octahedral, near-octahedral, and trigonal symmetry. *Chem. Phys. Lett.* **95**, 507-512 (1983).
22. Y. Hasegawa, M. Yamamuro, Y. Wada, N. Kanehisa, Y. Kai, A. Yanagida, Luminescent polymer containing the Eu(III) complex having fast radiation rate and high emission quantum efficiency. *J. Phys. Chem. A* **107**, 1697-1702 (2003).
23. A. Nakajima, T. Nakanishi, Y. Kitagawa, T. Seki, H. Ito, K. Fushimi, Y. Hasegawa, Hyper-stable organo-Eu^{III} luminophore under high temperature for photo-industrial application. *Sci Rep.* **6**, 24458 (2016).
24. H. Xu, Q. Sun, Z. An, Y. Wei, X. Liu, Electroluminescence from europium(III) complexes. *Cood. Chem. Rev.* **293-294**, 228-249 (2015).
25. L. Wang, Z. Zhao, C. Wei, H. Wei, Z Liu, Z. Bian, C. Huang, Review on the electroluminescence study of lanthanide complexes. *Adv. Optical Mater.* **7**, 1801256 (2019).
26. J. Kido, Y. Okamoto, Organo lanthanide metal complexes for electroluminescent materials. Chem. Rev. **102**, 2357 (2002).
27. M. Pietraszkiewicz, M. Maciejczyk, I. D. W. Samuel, S. Zhang, Highly photo- and electroluminescent 1,3-diketonate Eu(III) complexes with spiro-fluorene-xantphos dioxide ligands: synthesis and properties. *J. Mater. Chem. C* **1**,8028-8032 (2013).
28. H. Xu, K. Yin, W. Huang, Comparison of the electrochemical and luminescence properties of two carbazole-based phosphine oxide Eu^{III} complexes: effect of different bipolar ligand structures. *Chem. Phys. Chem.* **9**, 1752 (2008).
29. J. Wang, C. Han, G. Xie, Y. Wei, Q. Xue, P. Yan, H. Xu, Solution-processible brilliantly luminescent Eu^{III} complexes with host-featured phosphine oxide ligands for monochromic red-light-emitting diodes. *Chem. Eur. J.* **20**, 11137-11148 (2014).

30. D. B. A. Raj, S. Bijua, M. L. P, Reddy, 4,4,5,5,5-Pentafluoro-1-(9H-fluoren-2-yl)-1,3-pentanedione complex of Eu^{3+} with 4,5-bis(diphenylphosphino)-9,9-dimethylxanthene oxide as a promising light-conversion molecular device. *Dalton Trans.* 7519-7528 (2009).
31. H. Xu, L.-H. Wang, X.-H. Zhu, K. Yin, G.-Y. Zhong, X.-Y. Hou, and W. Huang, *J. Phys. Chem.* **110**, 3023-3029 (2006).
32. H. Xu, K. Yin, W. Huang, Novel light-emitting ternary Eu^{3+} complexes based on multifunctional bidentate aryl phosphine oxide derivatives: tuning photophysical and electrochemical properties toward bright electroluminescence. *J. Phys. Chem. C* **114**, 1674-1683 (2010).
33. M. Latva, H. Takalo, V.-M. Mukkala, C. Matachescu, J. C. Rodriguez-Ubisd, J. Kankarea, Correlation between the lowest triplet state energy level of the ligand and lanthanide(III) luminescence quantum yield. *J. Lumin.* **75**, 149-169 (1997).
34. S. Miyazaki, K. Miyata, H. Sakamoto, F. Suzue, Y. Kitagawa, Y. Hasegawa, K. Onda, Dual energy transfer pathways from an antenna ligand to lanthanide ion in trivalent europium complexes with phosphine-oxide bridges. *J. Phys. Chem. A* **124**, 6601-6606 (2020).
35. M. W. Mara, D. S. Tatum, A. March, G. Doumy, E. G. Moore, K. N. Raymond, Energy transfer from antenna ligand to europium(III) followed using ultrafast optical and x-ray spectroscopy. *J. Am. Chem. Soc.* **141**, 11071-11081 (2019).
36. C. Yang, L.-M. Fu, Y. Wang, J.-P. Zhang, W.-T. Wong, X-C. Ai, Y.-F. Qiao, B. S. Zou, L.-L. Gui, A highly luminescent europium complex showing visible-light-sensitized red emission: direct observation of the singlet pathway. *Angew. Chem., Int. Ed.* **43**, 5010-5013 (2004).
37. E. Kasprzycka, V. A. Trush, V. M. Amirkhanov, L. Jerzykiewicz, O. L. Malta, J. Legendziewicz, P. Gawryszewska, Contribution of energy transfer from the singlet state to the sensitization of Eu^{3+} and Tb^{3+} luminescence. *Chem. Eur. J.* **23**, 1318-1330 (2017).
38. A. Skumanich, M. Jurich, J. D. Swalen, Absorption and scattering in nonlinear optical polymeric systems. *Appl. Phys. Lett.* **62**, 446 (1993).
39. H. Kataoka, T. Kitano, T. Takizawa, Y. Hirai, T. Nakanishi, Y. Hasegawa, Photo- and thermo-stable luminescent beads composed of Eu(III) complexes and PMMA for enhancement of silicon solar cell efficiency. *J. Alloys Compd.* **601**, 293-297 (2014).
40. J. J. Snellenburg, S. P. Laptenok, R. Seger, K. M. Mullen, I. H. M. van Stokkum, Glotaran: A java-based graphical user interface for the R package TIMP. *Journal of Statistical Software* **49** *(3)*, 1-22 (2012).
41. J. Zhao, W. Wu, J. Sun, S. Guo, Triplet photosensitizers: from molecular design to applications. *Chem. Soc. Rev.* **42**, 5323-5351 (2013).
42. Z. An, C. Zheng, Y. Tao, R. Chen, H. Shi, T. Chen, Z. Wang, H. Li, R. Deng, X. Liu, W. Huang, Stabilizing triplet excited states for ultralong organic phosphorescence. *Nature Materials* **14**, 685-690 (2015).
43. M. H. V. Werts, R. T. F. Jukes, J. W. Verhoeven, The emission spectrum and the radiative lifetime of Eu^{3+} in luminescent lanthanide complexes. *Phys. Chem. Chem. Phys.* **4**, 1542-1548 (2002).
44. C. -G. Ma, M. G. Brik, D.-X. Liu, B. Feng, Y. Tian, A. Suchocki, Energy level schemes of f^N electronic configurations for the di-, tri-, and tetravalent lanthanides and actinides in a free state. *J. Lumin.* **170**, 369-374 (2016).
45. R. D. Spencer, G. Weber, Influence of Brownian rotations and energy transfer upon the measurements of fluorescence lifetime. *J. Chem. Phys.* **52**, 1654−1663 (1970).

46. M. Saigo, Y. Shimoda, T. Ehara, T. Ryu, K. Miyata, K. Onda, Characterization of excited states in a multiple-resonance-type thermally activated delayed fluorescence molecule using time-resolved infrared spectroscopy. *Bull. Chem. Soc. Jpn.* **95**, 381-388 (2022).

Acknowledgments

We acknowledge M. Uji and J. Kondo for their assistance with fluorescence lifetime measurements.

Funding: This work was partially supported by JSPS KAKENHI (grant numbers JP17H06375, JP18H05170, JP19K15508, JP20H05676, JP21K14590, JP20K21201, JP22H02152, JP22H04516, and JP22J11220), JSPS Core-to-Core Program (grant number JPJSCCA20180005), and the Iketani Science and Technology Foundation (ISTF). The computations were performed using the Research Centre for Computational Science (National Institute of Natural Sciences) and the Research Institute for Information Technology (Kyushu University). This work was supported by the Kyushu University Q-PIT Support Program for Young Researchers and Doctoral Students, and Young Researchers Support Project, Faculty of Science, KYUSHU UNIVERSITY Grant number 21-01 (R3) and 22-A5 (R4).

Author contributions: SM prepared the films. YK synthesized the complexes. KG and SM measured the optical properties of the sample. SM conducted the time-resolved spectroscopic measurements. KG and SM analyzed all the data. KO, KM, and SM drafted the original manuscript. KO and KM supervised the study. All authors contributed to the review and editing of the manuscript and critically commented on the project.

Competing interests: The authors declare that they have no competing interests.

Data and material availability: All data needed to evaluate the conclusions in the paper are presented in the paper and/or the Supplementary Materials.